Model-Based Analysis of Control/Display Interaction in the Hover Task

Sanjay Garg* and David K. Schmidt†
Purdue University, West Lafayette, Indiana

The effect of control/display interaction in the hover task is analyzed using an optimal control approach to modeling pilot control behavior. The control/display configurations considered are those previously evaluated in a flight research program. The experimental data base is reviewed, and the procedure for modeling the task and the displayed information is presented in detail. All model-based results, time-domain as well as frequency-domain, are found to correlate extremely well with with the subjective pilot ratings and comments. Time-domain measures consist of root mean-square errors and control inputs, attention allocation to displayed quantities, and magnitudes of task objective function. Frequency-domain measures include bandwidth, stability margins, and pilot phase compensation. Results are also shown to agree with previous findings on task interference in multiaxis tasks.

Nomenclature

$f_{()}$ = fraction of attention allocation to ( ) task
$g_{()}$ = weighting on rate of control ( )
p = body axis roll rate, deg/s
q = body axis pitch rate, deg/s
x,y,z = components of ground-referenced translation position, ft
$\dot{x},\dot{y},\dot{z}$ = components of ground-referenced translation rate, fps
J_p = model index of performance
$W_{()}$ = noise intensity in control channel ( )
δ_{ES} = longitudinal stick position, in.
δ_{CS} = collective stick position, deg
δ_{AS} = lateral stick position, in.
δ_{RP} = rudder pedal position, in.
$\epsilon_{()}$ = error in ( ) = commanded value minus actual value
ζ = damping ratio of second-order characteristic roots
θ = Euler pitch attitude, deg
θ_{WO} = washed-out pitch attitude signal, deg
τ = time constant of first-order response, s
τ_N = human's neuro-muscular lag time constant, s
τ_p = human's observation time delay, s
ϕ = Euler roll attitude, deg
ϕ_{WO} = washed-out roll attitude signal, deg
ψ = Euler yaw attitude, deg
ω_N = undamped natural frequency of second-order roots, rads/s
$()_c$ = commanded value of ( )
$()_m$ = maximum allowable value of ( )

Introduction

THERE is continued need to understand the interaction between display sophistication and control system complexity,[1] especially in terms of its effects on the pilot's performance and workload in multiaxis tasks. In Ref. 2 it was hypothesized that, for a given pilot rating, there exists an inverse relationship between control complexity and display with minimum stability augmentation or a high level of control augmentation with lesser display integration will be equally acceptable to the pilot. The hypothesis of Ref. 2 has been borne out in various experimental studies[3-5] conducted to investigate the display/control tradeoff in the vertical/short takeoff and landing (V/STOL) approach and landing task.

There are many approaches available to the control system designer for the design of flight control systems, but the techniques available for design of display systems are very limited in number. Display design techniques rely heavily upon mathematical models of pilot behavior and, since the development of an optimal control model (OCM) by Kleinman et al.,[6] various display design techniques based on this model have been suggested.[7-9] More recently, a methodology has been presented[10] that is intended to provide a systematic approach to synthesizing pilot-optimal control and display augmentation in complex, closed-loop, manual control tasks. This cooperative synthesis technique makes extensive use of an OCM, both for synthesis and analysis, and has as its basic premise the hypothesis that the value of the pilot's objective cost function J_p, as obtained from the model for a properly modeled task, is correlated with the pilot's subjective rating (PR).[11] Such a hypothesis has been corroborated using experimental data[12,13] for single-axis control tasks, and its extension to multiaxis tasks has been hypothesized. However, to the authors' knowledge, no extensive validation of the modeling procedure against experimental data, in which both the control system and the displayed information were variables, has been carried out.

If the OCM is to be useful as a *predictive design tool*, it is important that the model-based results reflect the qualities of the overall system when a simple performance index is chosen that represents a generic "critical" task. Also, all other model parameters cannot be adjusted a posteriori to match results. One objective of this study, then, is to determine whether not only the model performance index but also other model-based parameters are correlated with the pilot opinion rating when a simple modeling procedure is used. In addition, it is to be determined whether such a modeling procedure is appropriately sensitive to the display/control interaction known to be present. These objectives will be accomplished by performing a model-based evaluation of a set of experimental data. The data considered are those from Ref. 3, chosen because it consisted of an in-flight investigation involving combinations of

Presented as Paper 87-2287 at the AIAA Atmospheric Flight Mechanics Conference, Monterey, CA, Aug. 17-19, 1987; received June 23, 1987; revision received March 28, 1988.

*Ph.D. Candidate; currently, Control Engineer, NASA Lewis Research Center Group, Sverdrup Technology, Inc., Cleveland, OH. Member AIAA.

†Professor, School of Aeronautics and Astronautics; currently, Department of Aerospace Engineering and Engineering Mechanics, Arizona State University, Tempe, AZ. Associate Fellow AIAA.

various levels of display sophistication and control complexity. Moreover, detailed pilot comments were available, so the analytical and experimental results could be more meaningfully compared.

In the following, the experimental database to be used is first reviewed, and the control/display combinations to be analyzed are briefly discussed. The modeling procedure used in the analysis is then presented. The model-based time-domain results, consisting of values of the task objective function, root mean-square (rms) values of position errors and control activity, and attention allocation predictions, and frequency-domain results, using pilot describing functions derived from the model,[14,15] are then summarized. These time-domain and frequency-domain measures have been used previously in various model-based studies[16,17] to compare analytical and experimental results. Finally, these results are compared with the subjective pilot ratings and comments and discussed in detail to gain insight into the pilot/vehicle/display interaction in multiaxis tasks.

Experimental Data Base

A flight research program, undertaken to investigate control, display, and guidance requirements for vertical takeoff and landing (VTOL) aircraft in a steep approach to landing task under instrument meteorological conditions, is discussed in Ref. 3. The X-22A variable-stability aircraft was used for the experimental study. In all, 38 in-flight evaluations of combinations of 5 generic display formats and 5 levels of control augmentation systems were performed. Although the complete task considered was quite complicated, the design condition for both the display systems and control systems, as stated in Ref. 3, was precision hover. From the 38 cases considered in Ref. 3, 6 were selected for modeling, based on pilot comments indicating that hover was the task primarily affecting the ratings and that crosswind and turbulence were not a factor.

The display sophistication and control complexity for the six chosen configurations are shown in Fig. 1, along with the subjective PR. The spread in ratings (2–7, on a Cooper-Harper scale[11]) in Fig. 1 was wide enough for handling qualities analysis using the model. Note that, for the systems selected for model-based study, the hypothesized tradeoff between display sophistication and control complexity is evident for combinations rated adequate-but-unsatisfactory ($3.5 < PR < 6.5$). However, a rating of satisfactory ($PR < 3.5$) clearly requires a high level of sophistication in both the display and the control system. The three levels of control complexity and the two levels of display sophistication considered in Fig. 1 are discussed briefly in the following.

Control Systems

The basic airframe dynamics of the X-22A aircraft were modified using various augmentation schemes to yield generic levels of complexity. For all the systems, the characteristic dynamics were chosen to comply with MIL-F-83300[18] specifications for level I handling qualities at the hover condition. The vertical axis of the aircraft was unaugmented for all of the systems considered in the study.

1) RATE: This system consisted of pitch rate q feedback to the longitudinal stick δ_{ES}, roll rate p feedback to the lateral stock δ_{AS} and yaw rate r feedback into the rudder pedals δ_{RP}. This type of augmentation is the minimum stability augmentation system (SAS) considered feasible for V/STOL aircraft.

2) ATT: This system was implemented as pitch attitude command from the longitudinal stick and roll attitude command from lateral stick, using appropriate filters. The directional axis at hover was implemented as a yaw-rate-command-heading-hold system.

3) ATT/RATE: This was the same as ATT system for the pitch axis and the yaw axis. In the roll axis, this was implemented as a roll-rate-command-attitude-hold system.

The approximate attitude transfer functions for the three systems (as obtained from Ref. 3) are listed in Table 1. The aircraft dynamics are decoupled between the longitudinal and lateral-directional axes, while there was a small degree of coupling between the longitudinal and the collective input.

Display Systems

The primary instrument available to the evaluation pilot was a cathode ray tube (CRT) that presented integrated vertical and horizontal information. Other auxiliary information necessary for successful completion of the flight task was provided through various instruments such as an electromechanical attitude director indicator (ADI), airspeed indicator, and radar altimeter.

The symbology of the CRT display was designed using the guidelines of Ref. 19, so as to optimize the displays from a "human factors" point of view. The type of information available on this display was a variable in the experiment. The

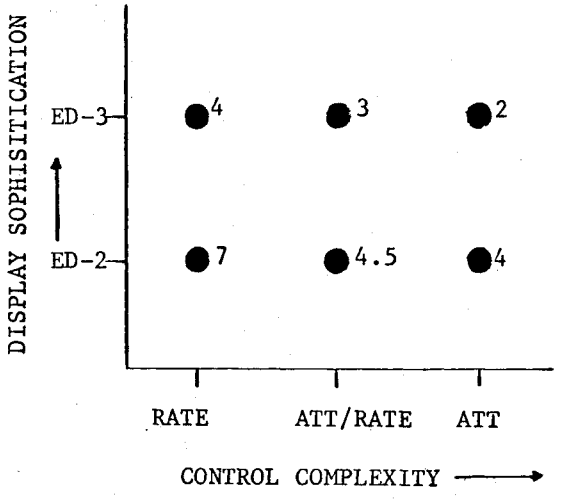

Fig. 1 Pilot rating for varying control/display combination.[3]

Table 1 Approximate attitude transfer functions (from Ref. 3)

$\{K(1/\tau)[\zeta,\omega_N] = K(s + 1/\tau)(s^2 + 2\zeta\omega_N s + \omega_N^2)\}$

System	θ/δ_{ES}	ϕ/δ_{AS}
RATE	$\frac{0.44(0.12)(0.14)}{(0.12)(2.94)[0.10;0.40]}$	$\frac{0.40(0.06)(1.74)}{(1.62)(2.71)[-0.025;0.45]}$
ATT	$\frac{[0.7;4.0]}{[0.7;2.0]} \cdot \frac{0.44(0.12)(0.14)}{(0.12)(0.17)[0.74;4.29]}$	$\frac{0.97(1.83)(2.16)(0.06)}{(0.16)(1.70)(2.48)[0.30;2.20]}$
ATT/RATE	$\frac{[0.7;4.0]}{[0.7;2.0]} \cdot \frac{0.44(0.12)(0.14)}{(0.12)(0.17)[0.74;4.29]}$	$\frac{(2)}{(0)} \cdot \frac{0.40(1.83)(2.16)(0.06)}{(0.17)(1.67)(2.60)[0.52;2.15]}$

two electronic display formats (ED-2 and ED-3) considered for this study are shown in Fig. 2. Apart from the unique information specific to each display, they both provide the following information: 1) aircraft pitch and roll attitude information, by means of a fixed aircraft symbol and a moving horizon bar, 2) horizontal position (x and y) of the aircraft with respect to the landing pad, by means of a moving pad symbol, 3) the heading of the aircraft with respect to the landing pad, by means of rotation of the landing pad symbol and a fixed aircraft tail symbol, 4) the heading-referenced ground velocity of the aircraft, by means of a velocity vector, and 5) the altitude error through an explicit symbol, and an expanding landing pad symbol.

Information specific to the ED-2 display was the altitude error rate and commanded horizontal velocity. The horizontal velocity command diamond is driven as follows:

$$\dot{x}_c = -0.19x_{\text{error}}, \qquad \dot{y}_c = -.057y_{\text{error}}$$

so that for a step position disturbance, the aircraft will return to hover in an exponential manner if the pilot keeps the tip of the velocity vector centered in the command diamond.

The ED-3 display consisted of a three-axes flight director including a horizontal bar (HBAR)—longitudinal stick (δ_{ES}) command; a vertical bar (VBAR)—lateral stick (δ_{AS}) command; and a vertical tab (VTAB)—collective stick (δ_{CS}) command. The logic driving the flight director signals was derived using the classical manual control theory.[20] The flight director logic is

$$\text{HBAR} = K_{\dot{x}}\epsilon_{\dot{x}} + K_\theta\theta_{WO} + K_q q$$

$$\text{VBAR} = K_{\dot{y}}\epsilon_{\dot{y}} + K_\phi\phi_{WO} + K_p p$$

$$\text{VTAB} = K_z\epsilon_z + K_{\dot{z}}\epsilon_{\dot{z}}$$

The values for the director gains varied as a function of the controlled vehicle characteristics, and were selected such that the director element response to the pilot's control input is like k/s in the anticipated region of crossover frequency.

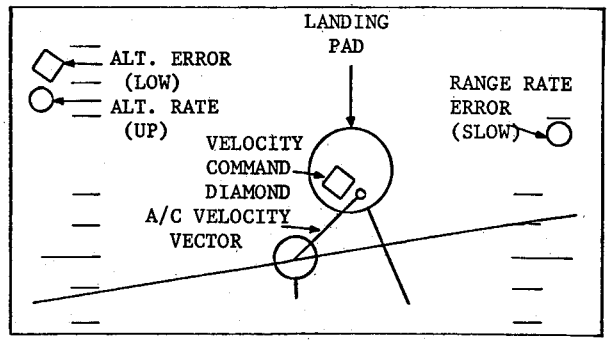

a) ED-2

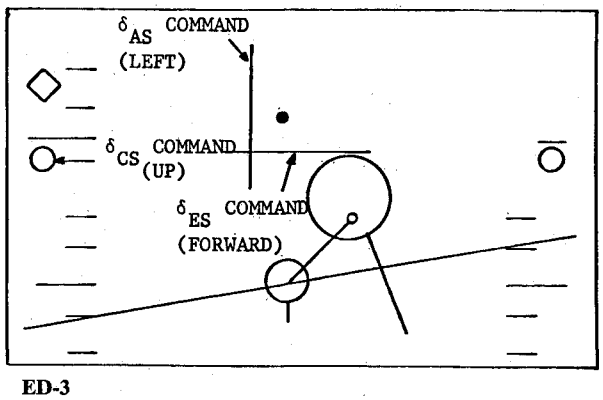

b) ED-3

Fig. 2 Electronic display formats.[3]

Task and Display Modeling

The task to be modeled is precision hover. Frequently, model-based studies of the hover task have considered velocity gusts to be the disturbance driving the aircraft.[9,12] However, as discussed earlier, pilot comments for the configurations being considered in this study indicate that turbulence was not a factor in determining the subjective rating. Because the aircraft's gust response is different from the response to pilot's control inputs, modeling the pilot's task as regulation in the presence of atmospheric disturbance is inappropriate here. It will be more appropriate to model the pilot's task as regulation against his own noise, or remnant.

In accordance with the modeling objectives discussed earlier, the performance index was chosen to simply represent the critical task of minimizing hover position error indicated on the display. The corresponding performance index is listed in Table 2. In Table 2, the maximum desirable values of the position errors x_m, y_m, and z_m were chosen to correspond to a displayed pad deflection of twice the human's observation

Table 2 Task modeling

$$J_p = J_{p_{\text{long}}} + J_{p_{\text{lat}}}$$

$$J_{p_{\text{long}}} = E\left[\lim_{T\to\infty}\frac{1}{T}\int_0^T\left\{\left(\frac{x}{x_m}\right)^2 + \left(\frac{z}{z_m}\right)^2 + \left(\frac{\delta_{ES}}{\delta_{ES_m}}\right)^2 + \left(\frac{\delta_{CS}}{\delta_{CS_m}}\right)^2 + g_{\delta_{ES}}\left(\dot{\delta}_{ES}\right)^2 + g_{\delta_{CS}}\left(\dot{\delta}_{CS}\right)^2\right\} dt\right]$$

$$J_{p_{\text{lat}}} = E\left[\lim_{T\to\infty}\frac{1}{T}\int_0^T\left\{\left(\frac{y}{y_m}\right)^2 + \left(\frac{\psi}{\psi_m}\right)^2 + \left(\frac{\delta_{AS}}{\delta_{AS_m}}\right)^2 + \left(\frac{\delta_{RP}}{\delta_{RP_m}}\right)^2 + g_{\delta_{AS}}\left(\dot{\delta}_{AS}\right)^2 + g_{\delta_{RP}}\left(\dot{\delta}_{RP}\right)^2\right\} dt\right]$$

(No rudder input for ATT/RATE and ATT systems)

x_m	= 12 ft	y_m	= 12 ft
z_m	= 8 ft	ψ_m	= 5 deg
δ_{ES_m}	= 1.4 in.	δ_{AS_m}	= 1.3 in.
δ_{CS_m}	= 5 deg	δ_{RP_m}	= 0.8 in.
$W_{\delta_{ES}}$	= $(0.2)^2$ in.^{2}	$W_{\delta_{AS}}$	= $(0.18)^2$ in.^{2}
$W_{\delta_{CS}}$	= $(0.1)^2$ deg^2	$W_{\delta_{RP}}$	= $(0.036)^2$ in.^{2}

$g_{(\,)}$ selected to yield $\tau_N = 0.2$ s in control channel ( )

Table 3 Observation vectors

Longitudinal		Lateral	
ED-2	ED-3	ED-2	ED-3
x	x	y	y
$\dot{x}$	$\dot{x}$	$\dot{y}$	$\dot{y}$
θ	θ	ϕ	ϕ
$\epsilon_{\dot{x}}$	HBAR	$\epsilon_{\dot{y}}$	VBAR
z	z	ψ	ψ
$\dot{z}$	VTAB		

Table 4 System performance for longitudinal task

System	x rms, ft	z rms, ft	θ rms, deg	δ_{ES} rms, in.	δ_{CS} rms, deg	$J_{p_{\text{long}}}$
RATE:ED-2	3.87	0.66	2.82	0.44	0.21	0.33
RATE:ED-3	2.41	0.50	2.10	0.40	0.20	0.24
ATT[a]:ED-2	1.49	0.39	1.08	0.34	0.21	0.15
ATT:ED-3	1.24	0.33	1.01	0.34	0.20	0.14

[a]ATT/RATE system is same as ATT system for longitudinal task.

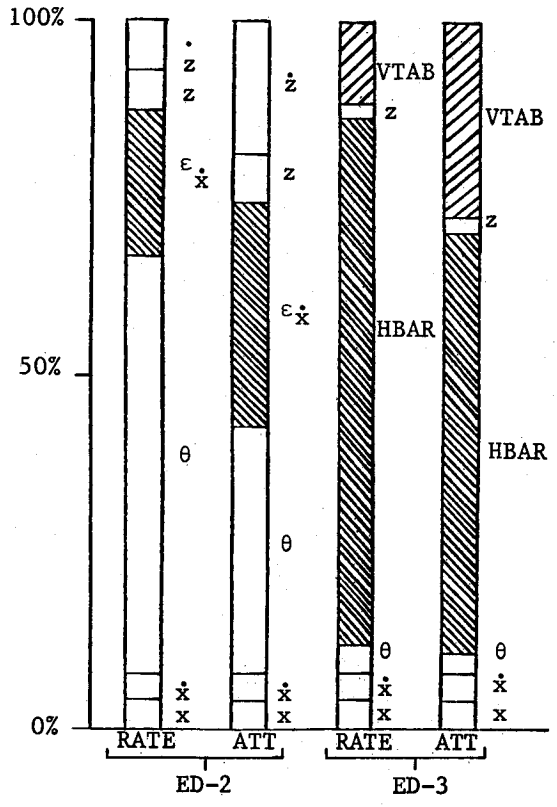

Fig. 3 Optimized fractions of attention for longitudinal task ($f_{long} = 0.5$).

threshold (a visual arc of 0.05 deg at the pilot's eye[21]). Such a choice reflects the requirement of precise control of position. The yaw attitude ψ was included in the task performance because for the RATE system there was no heading hold mode, and pilot's rudder control activity was required to maintain heading in hover. The value of ψ_m was chosen subjectively by the authors, considering 5 deg to be quite a large deviation. Based on the work in Ref 12, the maximum values of allowable control deflections were chosen to be one-quarter of the total control manipulator travel, and the weightings on the control rates were chosen to yield a neuromotor lag time constant τ_N of 0.2 s in each control channel.

Additive neuromotor noise was considered injected through the control manipulator by the pilot. The intensity of the noise for each control channel is also listed in Table 2. These noises, along with the observation noises, model the remnant, and they result in pilot's control noise to signal ratios of between -10 to -13 dB, considered reasonable for multiaxis human control tasks.

It is significant to note that the regulation of the flight director signals is *not* reflected in the index of performance. In a situation where both the status information and the director display signal is available, it is assumed that a well-trained, motivated pilot will use the director signal *only* if it helps him perform the critical task, which is reflected in the performance index. Minimizing errors involving the director signal in the index of performance directly is considered to lead to an improper model. The effect of the director display, then, appears only in the perception portion of the model, not in the task objective (index of performance). If a flight director signal truly aids the pilot's performance, then the model should indicate a large fraction of the pilot's attention being allocated to the flight director signal, even though the regulation of the

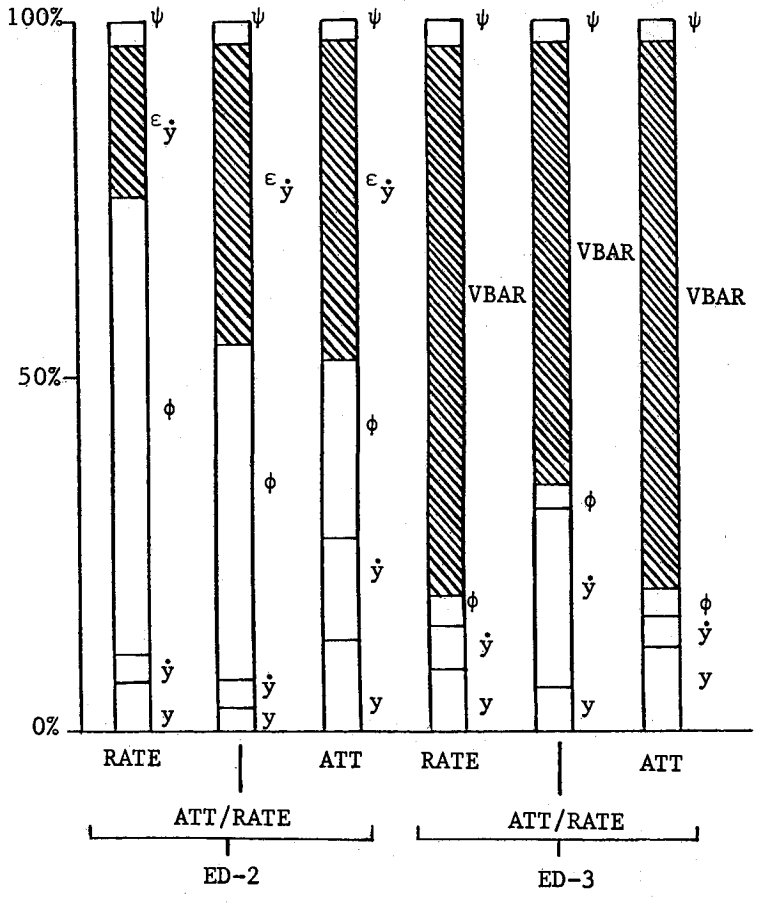

Fig. 4 Optimized fractions of attention for lateral task ($f_{lat} = 0.5$).

flight director signal is *not* explicitly included in the performance index.

The guidelines that were adopted in designing the displays in Ref. 3 are of importance when selecting the cues available to the pilot. Two of these guidelines are

(i) No attempt is made to have the pilot estimate absolute error or error rates implicitly by the rate of change of a position symbol on the display. When rates are displayed they are displayed explicitly.

(ii) The scaling of the various symbol motions is selected so as to be acceptable to the pilot while not significantly degrading overall system performance.

In view of these two guidelines, the pilot's observation vector was considered to consist of only the explicitly displayed variables, and the thresholds were chosen to be very low. The observation vectors for the longitudinal and lateral part of the task for the two displays being considered are listed in Table 3.

The observation time delay τ_p was chosen to be 0.2 s and the "full attention" noise to signal ratio was selected to be -20 dB for each observation. The pilot's full attention was assumed to be devoted to the control task, with the attentional allocation between the various observations optimized using the procedure in Ref. 9. In terms of attentional allocation between the longitudinal and the lateral tasks, it was found that an equal allocation of attention ($f_{long} = f_{lat} = 0.5$) led to best results (lowest value of J_p) for the systems being considered. This result is also consistent with the findings in Ref. 8.

Modeling Results

The time-domain model-based results of the rms values of the position variables (x, y, z), the attitude angles (θ, ϕ, ψ), and the control activity ($\delta_{ES}, \delta_{CS}, \delta_{AS}, \delta_{RP}$) are presented in Tables 4 and 5. The optimized allocations of attention are plotted in Figs. 3 and 4, shown as percentages of total attention in each axis. From Figs. 3 and 4 we note that a large part of the attention is in fact devoted to the flight directors for the ED-3 systems, indicating that the task performance, as modeled, is enhanced by the director display. This is also consistent with the pilot comments that the flight directors were very useful in accomplishing the control task. With reference to the modeling procedure discussed in the previous section (i.e., the regulation of flight directors *not* explicitly included in the task objective function), this result tends to confirm the validity of the modeling procedure, indicating that the procedure leads to results consistent with the crossover model,[22] the theory used to design the flight director logic.

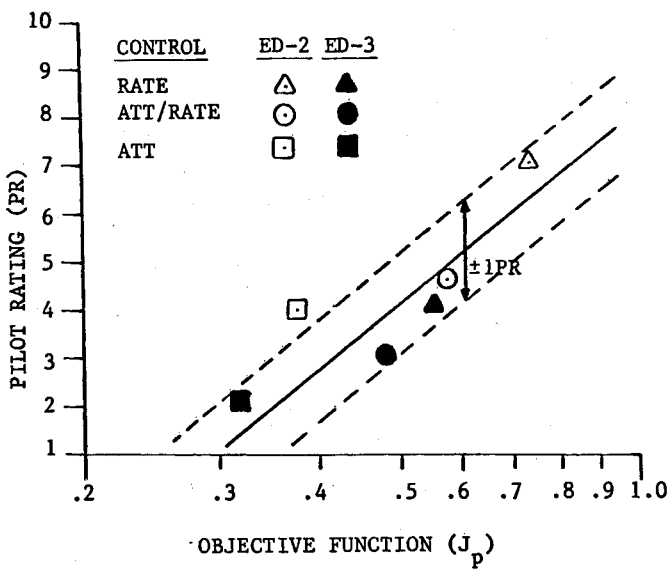

Fig. 5 Correlation between objective function J_p and pilot rating (PR).

The comparison between the magnitude of the objective function ($J_p = J_{p_{long}} + J_{p_{lat}}$) and the subjective PR for each configuration is summarized in Table 6. (The numbers in brackets are the pilot ratings on a Cooper-Harper scale). We note that, for a given type of display, as control complexity is increased (down the columns in Table 6) the pilot rating improves, and so does the value of the objective function, likewise for increased display sophistication (across the rows in Table 6). These results are also plotted in Fig. 5, showing the correlation between pilot rating and the value of the model objective function. Except for one configuration (discussed later) all of the other configurations lie within the ± 1 rating region. (Note that the straight line correlation shown in Fig. 5 is a hand-fit based on the results for just the six configurations being studied herein).

Frequency-domain analysis is also of fundamental importance in understanding the pilot/vehicle/display interaction. Furthermore, such an analysis helps tie in the optimal control model results with the crossover model.[22] As discussed earlier, the augmented vehicle dynamics being analyzed in this study are decoupled between the longitudinal and the lateral axes. Moreover, in the longitudinal axis, the coupling between the pitch and the collective input is deemed too small to be of major significance. Thus, the pilot's task will be considered here as three separate single-axis tasks. The generic block dia-

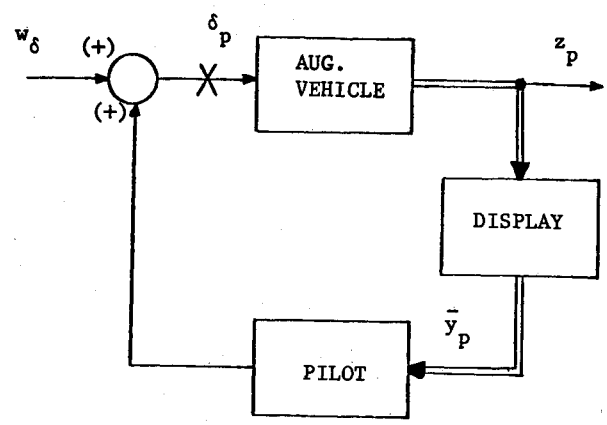

Fig. 6 Generic pilot/vehicle/display block diagram for each control input.

Table 5 System performance for lateral task

System	y rms, ft	ϕ rms, deg	ψ rms, deg	δ_{AS} rms, in.	δ_{RP} rms, in.	$J_{p_{lat}}$
RATE:ED-2	4.43	3.07	0.49	0.43	0.07	0.40
RATE:ED-3	3.33	2.34	0.44	0.39	0.07	0.31
ATT/RATE:ED-2	4.72	3.75	0.14	0.46	--	0.42
ATT/RATE:ED-3	3.86	3.01	0.11	0.42	--	0.34
ATT:ED-2	2.51	3.80	0.19	0.34	--	0.20
ATT:ED-3	1.95	3.45	0.18	0.33	--	0.18

Table 6 Comparison between objective function J_p and pilot rating (PR)

Control/Display	ED-2	ED-3
RATE	0.73[a]	0.55
	(7)[b]	(4)
ATT/RATE	0.57	0.48
	(4.5)	(3)
ATT	0.35	0.32
	(4)	(2)

[a] J_p. [b] PR.

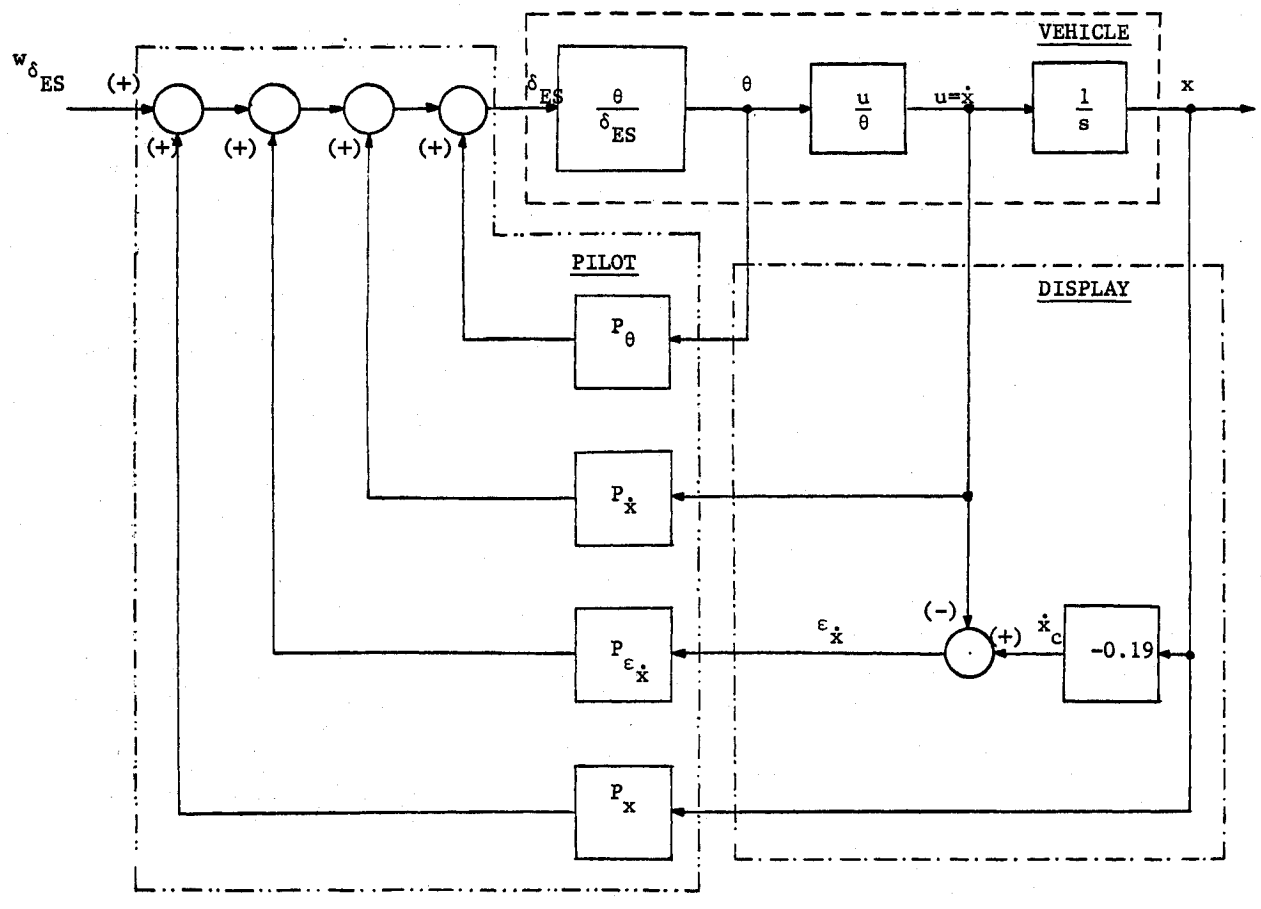

Fig. 7 Pitch axis pilot/vehicle/display block diagram for ED-2 display.

gram for the pilot/vehicle/display system *in each* axis (or control input) is shown in Fig. 6. In Fig. 6 w_δ corresponds to the modeled pilot remnant disturbing the vehicle, z_p is the controlled variable of interest for control input δ_p (e.g., x for δ_{ES}), and $\bar{y}_p$ is the vector of observed variables for this axis. The pitch-axis pilot/vehicle/display block diagram for the display format ED-2 is shown in Fig. 7 as one example of all the pilot loop closures considered in that axis. Analogous block diagrams could be considered in other axes. Frequency-domain representations of each of the blocks corresponding to the pilot ($P_{(\ )}$ in Fig. 7, for example) are obtained from the optimal control model, using the procedure in Ref. 6.

From an inspection of Figs. 6 and 7, it is clear that for a given control/display combination, measures of the quality of the overall loop closure—such as crossover frequency and stability margins—can be obtained by breaking the loop at the pilot output (or the vehicle input, marked X in Fig. 6). Examples of the loop-transfer function with the loop broken at the control input δ_{ES} are shown in Fig. 8 for the RATE:ED-2 and ATT:ED-2 systems. The loop-quality measures of crossover frequency ω_c, gain margin (G.M.) and phase margin (P.M.) are defined as shown. These δ_{ES} loop transfer functions for the RATE:ED-2 and ATT:ED-2 systems show that the magnitude slope at crossover is -20 dB/decade for both the systems. This was true of the loop-transfer functions for all of the three axes for the various control/display combinations considered in this study.

An important measure of pilot workload in the frequency domain is the pilot phase compensation at the loop crossover. But, since the pilot (model) in the systems being considered is multivariable (i.e., more than one input into the pilot for each control channel (see Figs. 6 and 7), the phase information can only be obtained from some form of an equivalent pilot compensation as, for instance, in Refs. 14 and 15. An inspection of Fig. 7 reveals that the individual pilot describing functions can all be reflected into a single equivalent pilot compensation at *any* of the inputs into the pilot model. The most meaningful way, however, is to consider the equivalent pilot describing function at the display variable providing primary command information to the pilot. These command signals are the velocity-error signals ($\epsilon_{\dot{x}}$, $\epsilon_{\dot{y}}$, $\epsilon_{\dot{z}}$) in the three axes for the ED-2 display format, and the three flight directors (HBAR, VBAR, VTAB) for the ED-3 display format. An example single-loop equivalent block diagram with equivalent pilot compensation in the pitch axis for the ED-2 display is shown in Fig. 9. Examples of the equivalent pilot describing functions are shown in Fig. 10 for the pitch axis of the RATE:ED-2 and RATE:ED-3 systems. Since the pilot describing functions in Fig. 10 include the effect of the modeled neuromuscular lag τ_N and the observation time delay τ_p, the model-based pilot phase compensation at crossover ($\measuredangle pc$) is defined as

$$\measuredangle pc = \measuredangle eq + 57.3\tau_p\omega_c + \tan^{-1}(\tau_N\omega_c)$$

In Fig. 8 ω_c was defined, and $\measuredangle eq$ is defined in Fig. 10 for the RATE:ED-2 system, for example.

The loop quality metrics and the equivalent pilot phase compensation for the three control channels δ_{ES}, δ_{AS}, and δ_{CS} and listed in Tables 7, 8, and 9, respectively. Considering the pitch axis (Table 7) first, note the low stability margins and the very high pilot lead compensation for the RATE:ED-2 system. Comparing the ED-2 systems with the ED-3 systems shows

that a major effect of providing the more sophisticated display (ED-3), for both the RATE and ATT systems, is to reduce the amount of pilot phase compensation. It is noted that this reduction in pilot work load is a major reason for improved pilot ratings with a more sophisticated display. As shown in Ref. 10 and elsewhere, improved performance (e.g., rms error) is almost a secondary effect. However, it is also interesting to note that the value of the objective function (as modeled) *is* sensitive to these effects (see Fig. 5).

Regarding the effect of control augmentation, we note from Table 7 that improving the vehicle dynamics not only leads to reducing pilot phase compensation, but also to a large improvement in stability margins. Although the improved display (ED-3) leads to improved margins, a dramatic improvement owing to attitude augmentation is evident. Not only are improved margins indicative of less susceptibility to pilot variations, but also low margins reflect high multitask workload. In Refs. 23 and 24, for example, high side-task workload was indicated in this fashion, and task interference was considered significant in cases having low stability margins.

The trends for the roll axis (Table 8) are similar to those discussed for the pitch axis. That is, the improved display leads to reduction in pilot phase compensation, whereas increased control augmentation brings about substantial improvement in the overall loop quality and reduction in pilot workload. However, it is interesting to note that the stability margins for the ATT/RATE system in the roll axis are just as bad as those for the RATE system, thus reflecting the difficulty of the lateral task here, as commented upon by the pilot ("Tendency to roll too much. . . ").

Considering the collective axis (Table 9), note that the major effect of increased control augmentation in the pitch axis (recall that the vertical axis dynamics are the same for RATE and ATT systems) is to increase the crossover frequency in the δ_{CS} loop and, hence, improve the performance in the vertical task. This result is consistent with the experimental findings in Refs. 23 and 24, wherein it is reported that the performance in the secondary task improved as the controlled dynamics in the primary task were made easier.

Interestingly, the results for the pitch axis and the roll axis (Tables 7 and 8) indicate that the loop crossover frequency is lower for the ATT systems as compared to the RATE systems, whereas the performance (rms errors) is much better for the ATT systems (see Tables 4 and 5). Although for a given closed-loop system, higher loop crossover frequency does indicate greater disturbance rejection, the issue here is that the two systems (RATE and ATT) respond very differently to external disturbances. For example, the forward position disturbance response to noise injected at the control input δ_{ES} (or remnant) is compared in Fig. 11 for the RATE and ATT systems. Note that the frequency content of the effective disturbance is much higher for the RATE system as compared to the ATT system. Therefore, the required pilot/vehicle loop crossover frequency to reject the disturbance is much higher for the RATE system than the ATT system.

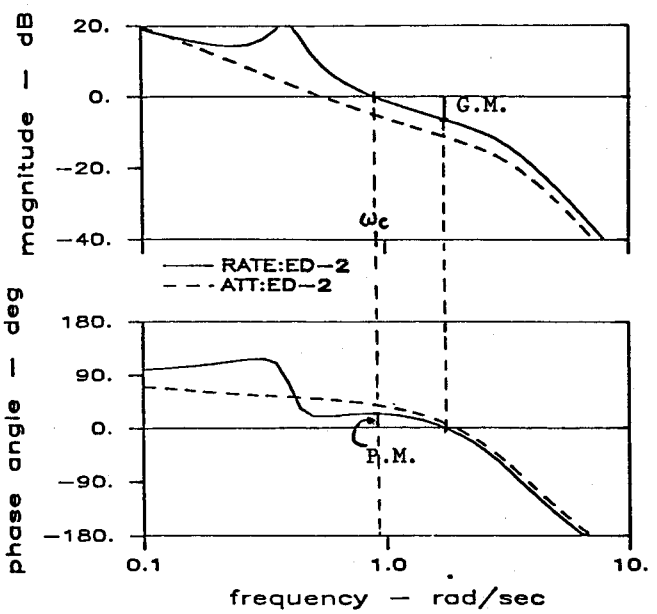

Fig. 8 Loop-transfer functions at control input (δ_{ES}).

Configuration Analysis

The comparison between the model-based time and frequency-domain results presented in the previous section, and the pilot comments from Ref. 3, is summarized below.

1) RATE:ED-2. Pilot comments indicate that attitude information is very important. ("Hard to get enough attitude

Table 7 Frequency-domain results—δ_{ES} loop

System	G.M., dB	P.M., deg	ω_c, rads/s	Δpc, deg
RATE:ED-2	6.3	24.0	0.93	68
RATE:ED-3	9.0	28.5	1.05	−9
ATT:ED-2	12.0	49.0	0.57	0
ATT:ED-3	13.5	44.6	0.68	−32

Table 8 Frequency-domain results—δ_{AS} loop

System	G.M., dB	P.M., deg	ω_c, rads/s	Δpc, deg
RATE:ED-2	6.0	22.8	0.95	63
RATE:ED-3	8.2	27.4	1.06	−30
ATT/RATE:ED-2	5.4	22.7	0.88	4
ATT/RATE:ED-3	8.0	29.5	1.07	−68
ATT:ED-2	8.6	43.5	0.71	−29
ATT:ED-3	11.2	49.5	0.85	−53

Table 9 Frequency-domain results—δ_{CS} loop

System	G.M., dB	P.M., deg	ω_c, rads/s	Δpc, deg
RATE:ED-2	12.5	48.0	0.60	−40
RATE:ED-3	11.0	43.0	0.75	−35
ATT:ED-2	10.0	40.5	0.85	−37
ATT:ED-3	10.0	39.2	0.95	−29

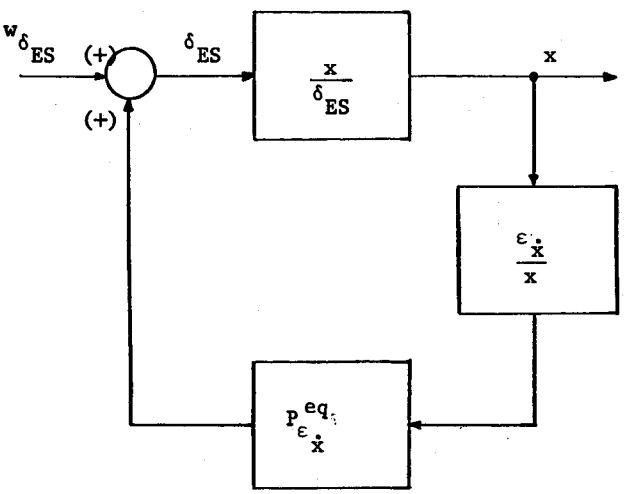

Fig. 9 Block diagram with equivalent pilot compensation (ED-2 pitch axis).

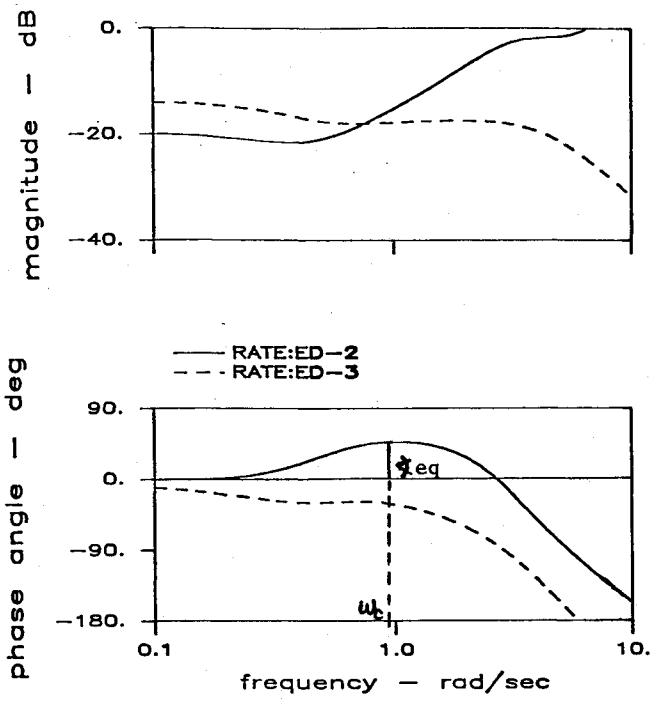

Fig. 10 Equivalent pilot describing functions in the pitch axis.

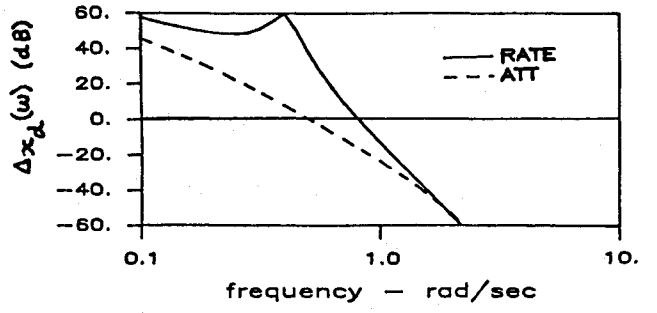

Fig. 11 Power spectra of disturbance response ($x_d/w_{\delta_{ES}}$).

information from electronic display. Performance very poor, got large attitudes trying to get to and stay over the spot.") Model-based results agree, indicating very high attention allocation to attitude angles θ and ϕ, and larger rms values of x, z, and θ than for all other systems. Also, the relatively large rms value of y and low stability margins, as compared to most other systems, agree with the pilot comment that "Poor attitude control makes airplane move left and right too quickly."

2) ATT/RATE:ED-2. The major pilot complaint was the difficulty of the lateral task. ("Tendency to roll too much when making lateral corrections.") This is reflected in the model-based results in terms of high value of $J_{p_{lat}}$ (slightly higher than RATE:ED-2, even), the high attention allocation to the roll attitude ϕ, and low stability margins.

3) ATT:ED-2. Although for this case the value of J_p would indicate a better pilot rating than obtained, the pilot phase compensation is higher than with ED-3. Moreover, pilot comments indicate that he was confused as to what to do with the altitude rate error circle and was scanning to the radar altimeter to help pick up lead on altitude. The pilot also seems to have had other concerns. For example, he states, "today we have to watch the engines closely since it's warm." It is speculated that some of these factors may have had a bearing on the degraded pilot rating for this particular configuration.

4) RATE:ED-3. Pilot comments about flight directors are, "Very good. Proper directions and very comfortable." The model-based result of almost all attention being devoted to the flight directors is consistent with these comments. Also, pilot comments indicate that pitch control was a problem in hover. The large rms value of θ for this system as compared to ATT:ED-3 and higher phase compensation in pitch than in roll reflect this difficulty.

5) ATT/RATE:ED-3. Pilot comments are, "A bit more attention to bank angle control is required than I'd like, is the biggest problem, is a mildly unpleasant deficiency." Although high attentional allocation to ϕ is not indicated, model-based results for this system show much higher attentional allocation to $\dot{y}$ as compared to that for the RATE:ED-3 and ATT:ED-3 systems. This implies that pilot compensation will be more than just closing the flight director (VBAR) loop.

6) ATT:ED-3. Pilot comments are, "A dream—good information, good control." Model-based results showing almost all attention being devoted to the three flight directors, low phase compensation, high stability margins, and good time-domain performance are all in agreement with these comments.

Therefore, not only is there a good correlation between the pilot rating and the value of the model objective function, but the other model results all *echo* the pilot comments.

Conclusions

Using an optimal control modeling approach, the display/control interaction in the hover task was analyzed for a set of VTOL vehicle configurations previously evaluated in a flight research program. A modeling procedure that consists of choosing the model objective function to reflect the simple, yet critical task of regulating hover position, with all model parameters set to "standard" values is suggested, and was found to lead to time and frequency-domain results consistent with the pilot comments. Model-based frequency-domain analysis revealed again that the major advantage of display augmentation is to reduce the pilot workload, while improvement in closed-loop (rms) performance is secondary. Control augmentation, when properly implemented, leads to both reduction in pilot workload and significant improvement in piloted system performance. All model-based frequency-domain results involving pilot compensation and loop-transfer functions were found to be consistent with the well-known crossover model.

The results of this study further enhance the applicability of the optimal control modeling approach, not only as an analytical tool to evaluate the handling qualities of piloted systems, but also to be used in model-based display/control design techniques.

Acknowledgment

This research was supported by the NASA Dryden Flight Research Facility, Ames Research Center under Grant NAG4-1. Mr. Donald T. Berry was the technical monitor. This support is gratefully appreciated.

References

[1]Fraser, D. C., "Flying Qualities," *Journal of Guidance, Control, and Dynamics* (special issue on Flying Qualities), Vol. 9, Sept.-Oct. 1986., p. 514.

[2]"V/STOL Displays for Approach and Landing," AGARD Rept. 594, Nov. 1972.

[3]Lebacqz, J. V. and Aiken, E. W., "A Flight Investigation of Control, Display and Guidance Requirements for Decelerating Descending VTOL Instrument Transition Using the X-22A Variable Stability Aircraft," Calspan, Buffalo, NY, Rept. AK-5336-F-1, Sept. 1975.

[4]Niessen, F. R. Kelly, J. R., Garven, J. F., Jr., Yenni, K. R., and Person, L. H., "The Effect of Variations in Controls and Displays on Helicopter Instrument Approach Capability," NASA TN D-8385, Feb. 1977.

[5]Franklin, J. A. Hynes, C. S., Hardy, G. H., Martin, J. L., and Innis, R. C., "Flight Evaluation of Augmented Controls for Ap-

proach and Landing of Powered-Lift Aircraft," *Journal of Guidance, Control, and Dynamics,* Vol. 9, Sept.-Oct. 1986 pp. 555-556.

[6]Kleinman, D. L., Baron, S., and Levison, W. H., "An Optimal Control Model of Human Response," Pts. I and II, *Automatica,* Vol. 6, May 1970, pp. 357-383.

[7]Levison, W. H., "A Model Based Technique for the Design of Flight Directors," *Proceedings of the Ninth Annual Conference on Manual Control,* NASA CR-142295 May 1973, pp. 163-172.

[8]Hess, R. A., "Analytical Display Design for Flight Tasks Conducted Under Instrument Meteorological Conditions," *IEEE Transactions on Systems, Man and Cybernetics,* Vol. SMC-7, June 1977, pp. 453-462.

[9]Hoffman, W. C., Kleinman, D. L., and Young, L. R., "Display/Control Requirements for Automated VTOL Aircraft," NASA CR-158905, ASI-TR-76-39, Oct. 1976.

[10]Garg, S. and Schmidt, D. K., "Cooperative Synthesis of Control and Display Augmentation," AIAA Paper 86-2204, Aug. 1986.

[11]Cooper, G. E. and Harper, R. P., Jr., "The Use of Pilot Rating Scale in the Evaluation of Aircraft Handling Qualities," NASA TN D-5153, April 1969.

[12]Hess, R. A., "Prediction of Pilot Opinion Ratings Using an Optimal Pilot Model," *Human Factors,* Vol. 19, No. 5, Oct. 1977, pp. 459-475.

[13]Schmidt, D. K., "On the Use of the OCM's Objective Function as a Pilot Rating Metric," *Proceedings of the 17th Annual Conference on Manual Control,* Los Angeles, CA, NASA CR-165005, June 1981, pp. 305-313.

[14]Bacon, B. J. and Schmidt, D. K., "An Optimal Control Approach to Pilot/Vehicle Analysis and the Neal-Smith Criteria," *Journal of Guidance and Control,* Vol. 6, Sept.-Oct. 1983, pp. 339-347.

[15]Anderson, M. R. and Schmidt, D. K., "Closed-Loop Pilot Vehicle Analysis of the Approach and Landing Task," *Journal of Guidance, Control, and Dynamics,* Vol. 10, March-April 1987, p. 187-194.

[16]Johannsen, G. and Govindaraj, T., "Optimal Control Model Predictions of System Performance and Attention Allocation and their Experimental Validation in a Display Design Study," *IEEE Transactions on Systems, Man and Cybernetics*, Vol. SMC-10, May 1980, pp. 249-261.

[17]Hess, R. A., "A Pilot Modeling Technique for Handling Qualities Research," AIAA Paper 80-1624, Aug. 1980.

[18]"Military Specification—Flying Qualities of V/STOL Aircraft," U.S. Army, MIL-F-83300, Dec. 1970.

[19]Young, L. R., "Integrated Display Principles and Some Applications to V/STOL Aircraft," *Proceedings of the 13th AGARD Guidance and Control Symposium on Guidance and Control Displays,* AGARD CP-96, 1971.

[20]Weir, D. H., Klein, R. H., and McRuer, D. T., "Principles for the Design of Advanced Flight Director Systems Based on the Theory of Manual Control Displays," NASA CR-1748, March 1971.

[21]Levison, W. H., "The Effects of Display Gain and Signal Bandwidth on Human Controller Remnant," Aerospace Medical Research Lab., Wright-Patterson AFB, OH, AMRL-TR-70-93, March 1971.

[22]McRuer, D. T. and Jex, H. R., "A Review of Quasi-Linear Pilot Models," *Transactions of Human Factors in Electronics,* Vol. HFE-8, No. 3, Sept. 1967, pp. 231-249.

[23]McDonnell, J. D., "Pilot Rating Techniques for the Estimation and Evaluation of Handling Qualities," Air Force Flight Dynamics Lab., Wright-Patterson AFB, OH, AFFDL-TR-68-76, Dec. 1968.

[24]Allen, W., Clement, W., and Jex. H., "Research on Display Scanning, Sampling and Reconstruction Using Separate Main and Secondary Tracking Tasks," NASA CR-1569, July 1970.